Appl. Phys. B 61, 333–338 (1995)

Applied Physics B Lasers and Optics

Imaging using hard X-rays from a laser-produced plasma

C. Tillman[1], A. Persson[1], C.-G. Wahlström[1], S. Svanberg[1], K. Herrlin[2]

[1] Division of Atomic Physics, Lund Institute of Technology, P.O. Box 118, S-221 00 Lund, Sweden
(Fax: + 46-46/222 42 50, E-mail: CARL.TILLMAN@fysik.lth.se)
[2] Department of Radiology, Lund University Hospital, S-221 85 Lund, Sweden
(Fax: + 46-46/11 69 56)

Received: 31 October 1994/Accepted: 11 May 1995

Abstract. Imaging of technical and biological objects using hard X-rays from a laser-produced plasma source is demonstrated. Magnification radiography and single-shot imaging of biological samples are feasible with the source, which utilised focused radiation from a short-pulse terawatt laser. Differential imaging with element specificity and a new projection geometry for X-ray radiography are proposed.

PACS: 07.85; 52.00

X-ray transillumination imaging is the most common machine-based diagnostic method in medicine [1]. One hundred years after the discovery of X-rays by Röntgen [2], diagnostic radiology has reached a very high level of sophistication [3]. In the present paper, medical and biological imaging using hard X-rays from a laser-produced ultra-intense plasma source is described, extending work recently reported [4]. Special features of this new type of imaging are ultra-sharp images and ultra-short exposure times. Further, spectroscopic imaging for element selectivity is discussed.

To reduce the risk of mutagenic transformations caused by the ionising radiation, it is very important to keep the X-ray dose as low as possible, especially in view of recent reports of hypersensibility to X-rays in a small fraction of the population [5]. The use of image plates with electronic read out allows a reduction of the X-ray dose compared to conventional X-ray film [6]. The use of optical non-ionising radiation for transillumination imaging employing different techniques for reducing the image blurring effects due to scattering has also attracted great interest [7–9]. However, at the present time it is not evident how useful such techniques will become, e.g., in mammographic applications.

The normal way of producing hard X-ray radiation is to send an energetic beam of electrons into a high-nuclear-charge (Z) material, normally tungsten or molybdenum. This results in the release of characteristic X-ray emission lines corresponding to the filling of inner-shell electron vacancies, and a Bremsstrahlung continuum. Medical X-ray imaging normally employs photon energies of about 20–100 keV to achieve adequate penetration through the body ($\approx$ 20 cm). Hard X-rays can also be produced by focusing intense laser radiation on a high-Z material [10]. Such generation becomes particularly efficient and interesting when employing an ultra-high intensity femtosecond laser (e.g. a table-top terawatt laser, T^3). It has been shown that a 0.3% efficiency of energy conversion from near-IR laser photons to X-rays with energies above 20 keV can be obtained [10]. Photon energies as high as 1 MeV can be generated. The pulse duration of the source is of the order of 1 ps [11].

We have recently shown that such a laser-produced X-ray source provides some unique features in imaging applications [4]. We could demonstrate radiography with a magnification factor of up to 80. This was possible by critically making use of the ultra-small size of the source, which was shown to be smaller than 60 μm using star imaging patterns. Further, we demonstrated a sufficient X-ray yield to allow single-pulse imaging using standard medical image plates.

In the present paper, we give further details on our set-up for X-ray imaging (Sect. 1) and give several image examples, including experimental-animal imaging (Sect. 2). Further, we discuss the applicability and utility of the new techniques (Sect. 3).

1 Experimental set-up

The laser used for the generation of X-rays is a 10 Hz table-top terawatt system based on chirped-pulse amplification in titanium-doped sapphire [12]. An Ar^+-laser-pumped mode-locked Ti:Sapphire oscillator provides 100 fs pulses which are stretched in time by a factor of about 2500 by the use of two gratings. Stretching the pulse in time before amplification keeps the pulse power low enough to allow small-sized amplifiers to be used without

optical damage. In the stretching process, different frequency components will be delayed correspondingly to their respective wavelength. These pulses are injected into a regenerative Ti:Sapphire amplifier via an intracavity Pockels cell. After amplification by a factor of 10^6 during 15 double passes, the pulses are switched out by the Pockels cell. Final amplification is achieved in a four-pass Ti:Sapphire amplifier pumped by about 1.3 J of green light from two Nd:YAG lasers. After final amplification, the diameter of the laser beam is increased to 50 mm in order not to damage optical components after temporal recompression. The pulses are recompressed to 150 fs in a grating arrangement, reversed compared to the stretcher. The short pulse duration together with the pulse energy of up to 220 mJ gives peak powers of more than 1 TW. An overview of the laser system is shown in Fig. 1a.

Via two gold-coated $\lambda/10$ beam-steering mirrors the laser beam is directed into a vacuum chamber. Inside the vacuum chamber the 50 mm diameter laser beam is focused by an $f/1$ off-axis parabolic mirror to a diameter of the order of a few μm. Refractive optics (lenses) with low f numbers are not suitable for focusing due to the nonlinear refractive index of the material at the very high peak intensities present, resulting in self-phase-modulation rapidly destroying the pulse temporally and spatially.

The focusing mirrors used are $\lambda/4$ gold-coated aluminium substrates (Janos Technology, USA). Focused intensities beyond 10^{18}W/cm^2 can be achieved. A disc of 0.25 mm thick tantalum foil is placed in the focus. Every laser pulse creates a dense plasma, burning a small crater in the target foil. The foil is glued to a steel disc which is slowly rotated and translated in such a way that every new laser pulse hits a fresh spot on the surface (Fig. 1b). Depending on the separation between the craters, one such disc will last for one or two hours of operation at 10 Hz. The ablated target material is deposited on the interior of the chamber as well as on the focusing optics. Light particles are decelerated by operating with a background pressure of about 30 mbar of air in the vacuum chamber. These particles therefore do not stick onto the surface of the focusing mirror but can easily be removed by an air blow after opening the chamber. However, heavy particles of more than 10 μm diameter are permanently attached to the unprotected mirror surface. After a few hours of operation the mirror needs to be repolished and recoated. Thin plastic or glass pellicles have also been successfully used about 2 cm in front of the target surface, in order to prevent direct sputtering on the mirror surface.

Preliminary measurements of the energy distribution from a tantalum plasma have been performed. These measurements were done using energy dispersive NaI and Ge detectors in a single-photon counting mode and long acquisition times. Characteristic emission lines, in particular the K_α and K_β lines at 57 and 65 keV, respectively, as well as a broad Bremsstrahlung distribution were observed.

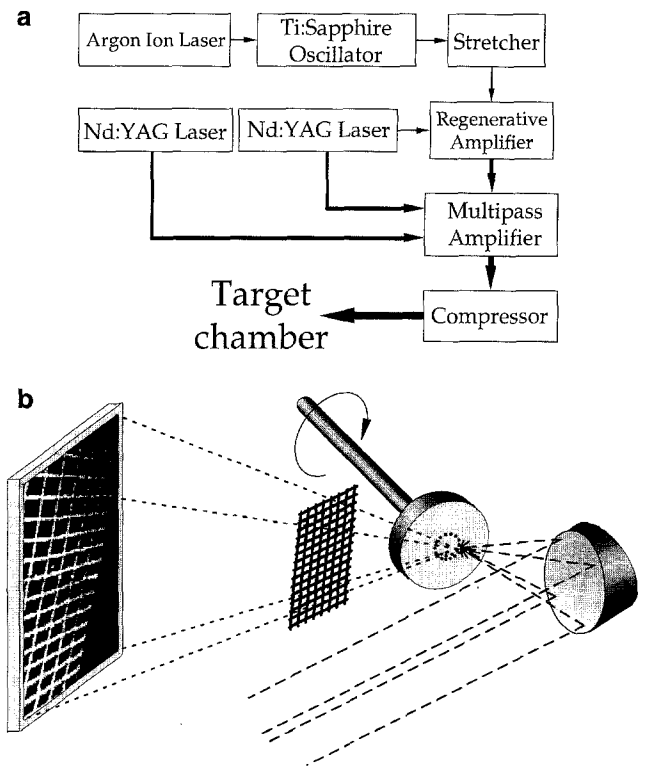

Fig. 1. a Laser system overview: An Ar^+ laser pumping a Ti:Sapphire oscillator provides 100 fs pulses which, after stretching by a factor of 2500 in time, are fed into a regenerative amplifier. After final amplification in a multipass unit, the pulses are compressed in time to a pulse length of 150 fs and a peak power of 1.5 TW. **b** Target chamber overview: The 50 mm diameter laser beam is focused inside a vacuum chamber by an off-axis parabolic mirror onto a high Z target surface. The radiation from the laser-produced plasma is utilised for image recording on image plates

2 X-ray imaging

For the applications presented here, image plates have been used as the recording device [6, 13]. These plates, now commonly used in medical radiology, are composed of a photo-stimulable crystal layer on a plastic substrate. The crystal layer consists of europium-doped barium-fluorohalide compounds. During X-ray exposure, the energy absorbed is stored in colour centres, where electrons are trapped in empty lattices of the fluorine and halide ions. The plates can be scanned, up to several hours after exposure, with a HeNe laser (633 nm) exciting the photo-stimulable layer and thus releasing the energy from the stored image by emitting luminescence light with a wavelength of about 400 nm. The emitted light is detected with a photomultiplier tube. After amplification, the signal is digitised, and the digital images thus created can easily be further processed numerically. The image plates exhibit a number of advantages:

- Ultrahigh sensitivity compared to films;
- A dynamic range of 10^4–10^5, compared to films with a dynamic range of about 10^2;
- A linearity far exceeding that of a film;
- Before exposure any accumulated background can be erased;
- Image plates can be reused after erasure of the previously recorded image.

The plasma generation has to be done at strongly reduced pressure, and a 0.2 mm polyethylene film was used as a vacuum-proof exit window for the generated X-rays. Soft X-rays are absorbed in this window but at 10 keV or above, the absorption was less than 10%. During exposure, wet samples have to be left at atmospheric pressure, while dry samples can be inserted in the vacuum chamber. The image plates can be placed either inside the chamber or outside. Since visible light erases the recorded image, the plate itself has to be covered with an opaque black plastic film.

The exposure time can be varied from a single laser shot up to several minutes. For each laser shot the exposure time is estimated to be of the order of picoseconds. One minute of operation is therefore corresponding to an effective exposure time of less than a nanosecond. Long exposure times will result in slightly blurred exposures because of mechanical imperfections resulting in slight wobbling of the rotating target. Single-shot exposures will, of course, totally eliminate this type of blurring as well as blurring caused by motion of the object being imaged. However, due to the limited number of photons per pulse, single-shot recordings can only be used for thin samples and short target/image-plate distances. Figure 2 shows a human Incus as well as a copper mesh recorded with one single laser pulse without any filter in front of the object. In this recording, the distance between the plasma and the object was ≈ 1 cm, and the distance between the plasma and the image plate was ≈ 10 cm. The estimated exposure in this case corresponds to an absorbed X-ray dose in water, at the position of the object, of about 1 Gy.

The high penetration depth of the X-rays can be seen in Fig. 3. These images, exposed during several minutes, show fine details through a steel watchcase (Fig. 3a) and through an IC-socket casing (Fig. 3b). In order to obtain good contrast in biological samples, with a reasonable X-ray dose, the X-ray photon energy should be optimised with respect to the thickness. In medical imaging, photon energies in the range 10–100 keV are normally used, with the higher energies for thicker samples. The effect of prefiltering can be seen in Figs. 4a and b, showing a Wistar-Furth rat. The image in Fig. 4a was recorded without any additional filter and the image of Fig. 4b was filtered with a 0.15 mm copper foil with a 90% X-ray absorption at 25 keV. The exposure times were 5 and 10 min, and the absorbed doses were estimated to be of the order of 1 Gy, but with a reduction of a factor two for the exposure with the copper filter. Since the low-energy part of the radiation is attenuated, the filtered image of this relatively thin object (≈ 3 cm) shows less contrast. Another example of biological imaging is shown in Fig. 5. A 4 day old Syrian hamster is shown with much structure on this image, although the skeleton parts have still not mineralised.

The present focusing optics offer a theoretical spot size of the focused laser radiation of about one micron in diameter. With a HeNe laser it has been measured to less than 2 μm in reality. Measurements with a star test pattern have shown that the X-ray emitting spot is less than 60 μm. A very small emitting spot size enables ultra sharp imaging and magnification during exposure. With a small enough spot, projection microscopy can be done. In Fig. 2, also the magnification aspect is shown. Since the distance from the plasma is not constant for all parts of the object, the magnification factor varies in this case between 10 and 15.

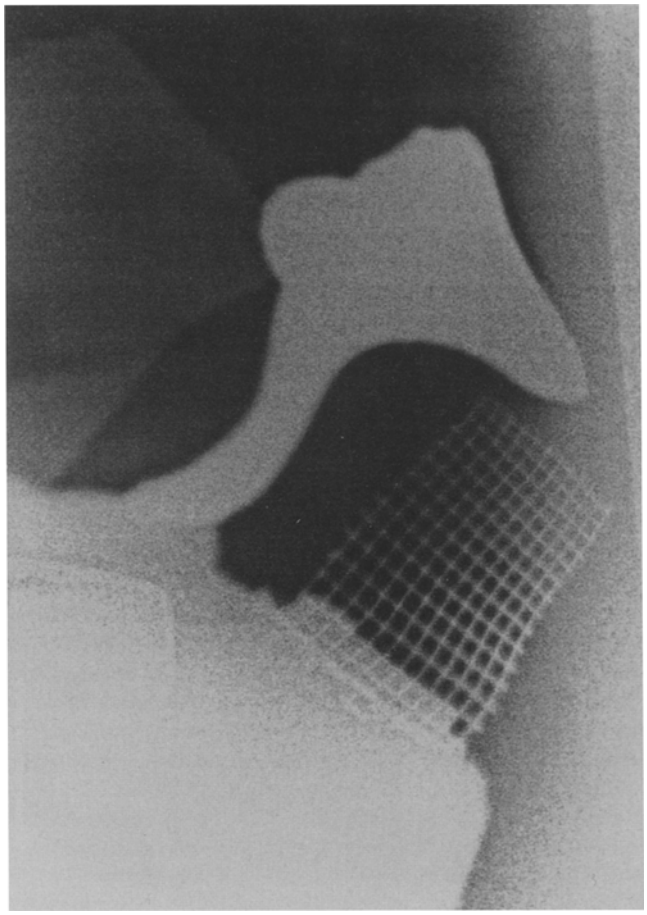

Fig. 2. Image of an Incus and a copper mesh (100 lines per inch) exposed by a single laser shot with a magnification of 10–15 times

3 Discussion

As discussed in Sect. 1, the ablated material from the target is a problem. Electron microscopy images of thin glass plates exposed to the sputtering target show particles of the size 1–10 μm. Thin pellicles of nitro cellulose, mylar, or glass have been used for protection of the focusing mirror. Even though thin pellicles might work as an alternative for the protection of the optics, the problem still remains of changing pellicles during a long time exposure. Another option would be to use a rotating chopper, letting through the laser pulse but stopping most of the ablated particles [14].

The very high temporal resolution might be difficult to fully exploit in biological imaging, since most processes on the cell scale occur in a much longer time frame. However, in medical imaging it is always of great concern to keep the X-ray dose as low as possible for the patients. One way of utilising the high time resolution would be to gate a very fast X-ray-sensitive camera in order to suppress multiple-scattered X-ray photons. It has been estimated

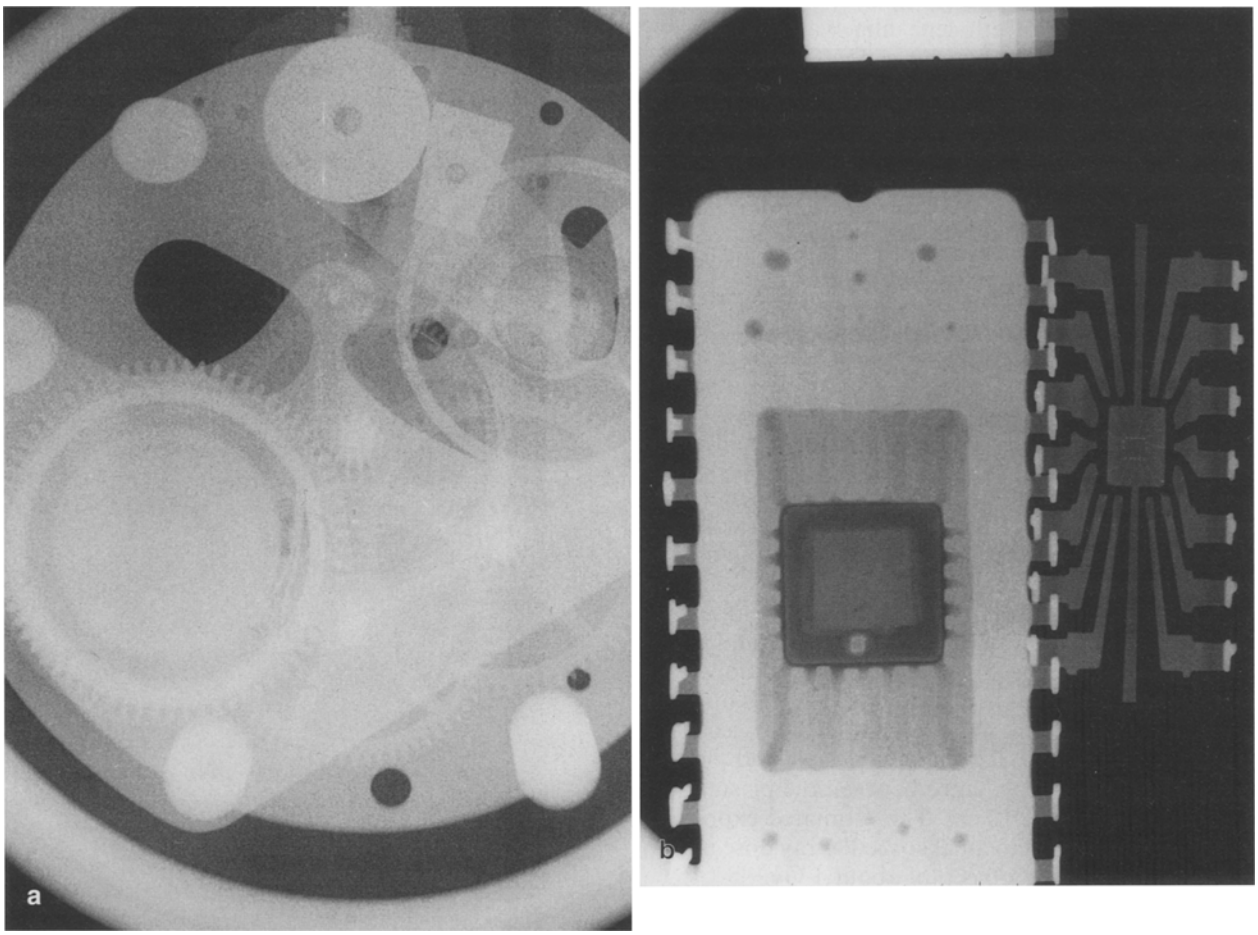

Fig. 3. **a** Image of a mechanical stop watch in a steel casing, magnified by a factor of 4.1 and exposed at 10 Hz during 10 min. **b** Image of integrated circuits, an EPROM memory capsule (*left*) and a standard DIL socket (*right*). Exposed at 10 Hz during 5 min

that the dose reduction could be as high as a factor of 8 using this technique [15].

X-ray photons are considered hazardous partly because of their ability to break DNA bonds. It is not clear how the time duration of the pulses is correlated to this kind of radiation damages. Living tissue has the possibility to repair most of these broken DNA bonds. For conventional X-ray sources with a pulse length of the order of milliseconds or microseconds, this healing process is usually fast enough so that only single-bond breakings occur. In our case, the X-ray pulse is extremely short, of the order of a few ps, and the number of photons per unit time will be about 10^6–10^9 times higher for the same dose. This may cause more than one bond to break on the same DNA molecule. Thus, the biological response to a given dose of this new type of ultra-intense X-ray pulses may be different compared to that for standard sources. It is also possible that standard methods of measuring X-ray exposure yield different values and thus are not applicable on this new type of X-ray source. These questions need to be addressed.

Conventional X-ray tubes do not enable the X-ray source to be placed inside the object of examination. Since high voltage has to be applied to the target, it is difficult to make it small. With the laser-generated X-ray source it would be feasible to design the target as a small pellet or a moving wire at the tip of an evacuated cone. This geometry would allow new image projections. As an illustration, the X-ray source could be placed inside the body of a rat with a cylindrical projection of the rat recorded on an image plate wrapped around the body (Fig. 6). This technique might apply to certain human cavities.

Subtraction imaging is a well-known technology within medical angiography [16, 17]. Usually, this is performed by injecting an iodine-based contrast medium in the blood vessels, simultaneously watching live X-ray images on an X-ray image intensifier. Images can be stored digitally, using a frame grabber. By subtracting the intensities in two such images pixel by pixel, where one image is taken immediately before the injection and the other one after the injection, one can achieve a high-contrast image of the blood vessels. Another kind of subtraction imaging employs two images exposed at different voltages applied to the X-ray tube. In a conventional X-ray tube, the maximum energy in the Bremsstrahlung spectrum is directly depending on the voltage across the tube. With this technique, bones can be filtered out of an image to improve the contrast of soft tissue, or vice versa. Both

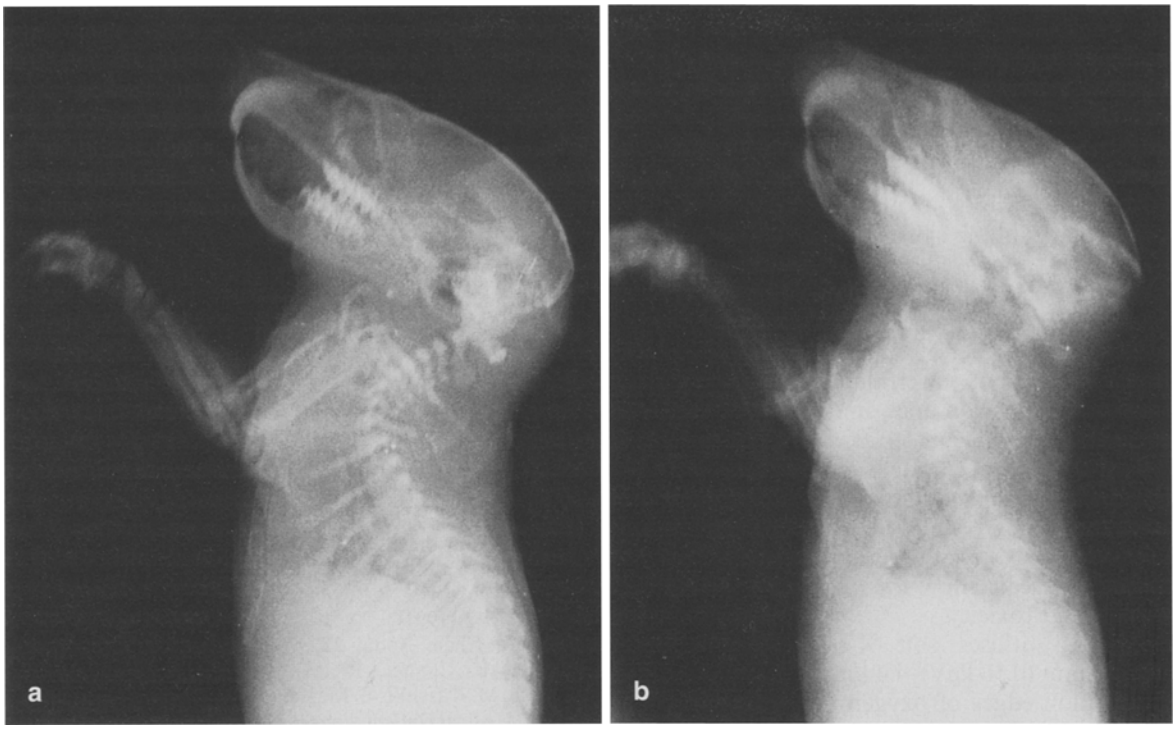

Fig. 4. **a** Wistar-Furth rat exposed at 10 Hz during 5 min without any additional filter. **b** Wistar-Furth rat exposed at 10 Hz during 10 min through a 0.15 mm copper filter, absorbing > 90% of the X-ray photons below 25 keV. Note that part of the fine details have been lost due to a higher average photon energy compared to the unfiltered image

Fig. 5. Magnified (×3.7) image of a 4 day old Syrian hamster. Exposed at 10 Hz during 5 min

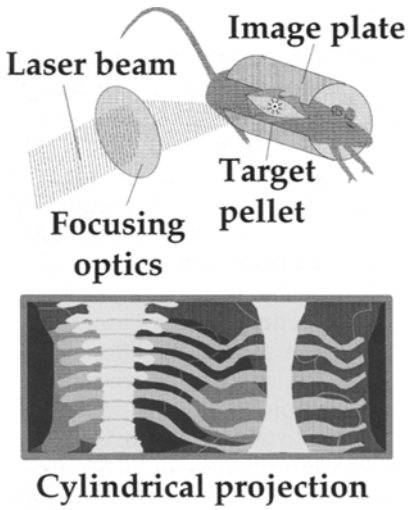

Fig. 6. Example of a proposed new image projection made possible by laser-assisted X-ray generation: A cylindrical projection of an object is made possible by placing the X-ray source inside the object under investigation and the recording medium wrapped around it

conventional X-ray tubes and laser-produced plasmas emit X-rays as continuous Bremsstrahlung and as discrete characteristic line emission, the latter depending on the atomic number of the target element. Preliminary measurements of the energy distribution of X-rays, in the energy range 40–80 keV, from the laser-produced plasma, and from a conventional X-ray tube were performed using

a calibrated Compton scattering spectrometer. These measurements indicate a larger relative amount of characteristic line emission from our laser-generated X-ray source than from the conventional source. Changing the target element affects the characteristic line emission energies. Since these lines are extremely sharp, subtraction imaging using different target elements offers a higher contrast compared to conventional exposures where the upper limit of the Bremsstrahlung spectra is altered.

Gadolinium has been approved for clinical use as a paramagnetic contrast medium in magnetic resonance imaging. The X-ray absorption is higher than the absorption in iodine, because of its higher atomic number. With gadolinium as a contrast medium, the elements suitable as target elements, with their emission lines on either side of the gadolinium K absorption edge at 50.2 keV, would be gadolinium itself on the lower side, and tantalum ($K_\alpha = 57$ keV) as the most practical choice on the upper side. Energies around 50 keV are suitable concerning the penetrating characteristics of these energies in bone and soft tissue. This technique can allow for a reduction of contrast-medium dose and toxicity.

Microscopic imaging utilises soft X-rays, in the wavelength range 2.2 nm (0.56 keV)–4.4 nm (0.28 keV), between the K absorption edges of oxygen and carbon, respectively, where a natural contrast between proteins and water is obtained [18]. For this kind of applications, possible attractive alternatives to normal electron bombardment production are emerging, e.g., X-ray lasers [19] or high-order harmonics of intense laser radiation [20, 21]. However, such processes are not likely to be able to produce sufficiently energetic X-rays to be useful in normal diagnostic radiology in medicine.

Measurements of the spectral distribution of the emitted radiation from a laser-produced plasma, with energy-dispersive detectors such as sodium–iodine and germanium detectors, are associated with pile-up effects. The dead time for these detectors limits the measurement to one X-ray photon for each laser shot, and, consequently, very long data-acquisition time. As a remedy, multielement detectors such as CCD arrays can be used [22]. Wavelength dispersive detectors can normally only be used for measuring X-rays with energies below ≈ 20 keV.

Measurements of absorption in foils of different elements is another approach for spectral measurements. The position of the K absorption edge for different elements range from 13.6 eV up to about 115 keV for the heaviest elements. Varying the thickness of two foils of different elements, the absorption curve of the two foils can be matched so that they almost coincide except in the range between the corresponding K absorption edges. Arranging a number of foils in a small matrix would make it possible to measure the absorption in all of the foils simultaneously in one exposure on an image plate. Subtracting the exposure values, two by two, gives the relative intensity in the different energy intervals [23].

Acknowledgements. Valuable discussions with S. Borgström, B. Erlandsson, C. Olsson, H. Pettersson, and G. Svahn are greatly acknowledged. This work was supported by the Swedish Natural Sciences Research Council, the Swedish Medical Research Council and the Crafoord Foundation. The project is part of the EC Human Capital and Mobility Programme (CHRX-CT93-0346).

References

1. R.S. MacKay: *Medical Images and Displays: Comparisons of Nuclear Magnetic Resonance, Ultra-Sound, X-Rays and Other Modalities* (Wiley, New York 1984)
2. W.C. Röntgen: Sitzungsber. Physikal.-Medizin. Ges. **132** (Würzburg 1895) [English transl. Nature **53**, 274 (1896)]
3. T.S. Curry III, J.E. Dowdey, R.C. Murry Jr: *Christensen's Physics of Diagnostic Radiology*, 4th edn. (Lea & Febiger, Philadelphia 1990)
4. K. Herrlin, G. Svahn, C. Olsson, H. Pettersson, C. Tillman, A. Persson, C-G. Wahlström, S. Svanberg: Radiology **189**, 65 (1993)
5. M. Swift, D. Morrell, R.B. Massey, C.L. Chase: New Engl. J. Med. **325**, 1831 (1991)
6. J. Miyahara: Chem. Today **223**, 29 (1989)
7. G. Müller, B. Chance, R. Alfano, S. Arridge, J. Beuthan, E. Gratton, M. Kaschke, B. Masters, S. Svanberg, and P. van der Zee (eds): *Medical Optical Tomography: Functional Imaging and Monitoring* (SPIE, Bellingham, VA 1993) Vol. IS11
8. S. Andersson-Engels, R. Berg, S. Svanberg, O. Jarlman: Opt. Lett. **15**, 1179 (1990)
9. R. Berg, O. Jarlman, S. Svanberg: Appl. Opt. **32**, 574 (1993)
10. J.D. Kmetec, C.L. Gordon III, J.J. Macklin, B.E. Lemoff, G.S. Brown, S.E. Harris: Phys. Rev. Lett. **68**, 1527 (1992)
11. P. Nickles: Private communication (1994)
12. S. Svanberg, J. Larsson, A. Persson, C.-G. Wahlström: Phys. Scr. **49**, 187 (1994)
13. M. Sonada, M. Takano, J. Miyahara, H. Kato: Radiology **148**, 833 (1983)
14. M. Schulz, A. Michette, R. Burge: In [18] pp. 58–62
15. C.L. Gordon III, C.P.J. Barty, S.E. Harris: In *Ultrafast Phenomena* IX, Springer Ser. Chem. Phys., Vol. 60 (Springer, Berlin, Heidelberg 1994) pp. 278
16. W.R. Brody: *Digital Radiography* (Raven, New York 1984)
17. P. Maher, J.F. Malone: Contemp. Phys. **27**, 533 (1986)
18. A.G. Michette, G.R. Morrison, C.J. Buckley (eds): *X-ray microscopy III*, Springer Ser. Opt. Sci., Vol. 67 (Springer, Berlin, Heidelberg 1992)
19. D. Matthews, D. Eder (eds): *X-Ray Lasers* (AIP, New York 1994)
20. A. L'Huillier, L.A. Lompré, G. Mainfray, C. Manus: In *Atoms in Intense Laser Fields*, ed. by M. Gavrila (Academic, San Diego 1992)
21. C.-G. Wahlström, J. Larsson, A. Persson, T. Starczewski, S. Svanberg, P. Salières, Ph. Balcou, A. L'Huillier: Phys. Rev. A **48**, 4709 (1993)
22. D.H. Lumb, G.R. Hopkinson, A.A. Wells: Nucl. Instrum. Methods **221**, 150 (1984)
23. C. Tillman, A. Persson, C.-G. Wahlström, S. Svanberg: *High Field Interactions and short Wavelength Generation*, OSA Tech. Dig. Ser., Vol. 16 (Opt. Soc. Am., Washington, DC 1994)